

LATE PLEISTOCENE AND EARLY HOLOCENE WINTER AIR TEMPERATURES IN KOTELNY ISLAND: RECONSTRUCTIONS USING STABLE ISOTOPES OF ICE WEDGES

Yu.K. Vasil'chuk^{1,2}, V.M. Makeev³, A.A. Maslakov¹, N.A. Budantseva¹, A.C. Vasil'chuk¹

¹ Lomonosov Moscow State University, Faculty of Geography and Faculty of Geology, 1, Leninskie Gory, Moscow, 119991, Russia

² Tyumen State University, 6, Volodarskogo str., Tyumen, 625003, Russia; vasilch_geo@mail.ru

³ Russian State Hydrometeorological University, 98, Malookhtinsky prosp., St. Petersburg, 109017, Russia

Late Pleistocene and Holocene winter air temperatures in Kotelny Island, northeastern Russian Arctic, have been reconstructed using oxygen isotope compositions of ice wedges and correlated with evidence of Late Pleistocene and Holocene climate variations inferred from pollen data. The $\delta^{18}\text{O}$ values range exceeds 6 ‰ in Late Pleistocene ice wedges but is only 1.5 ‰ in the Holocene ones (–30.6 ‰ to –24.0 ‰ against –23.1 ‰ to –21.6 ‰, respectively). The Late Pleistocene mean January air temperatures in Kotelny Island were 10–12 °C lower than the respective present temperature. On the other hand, mean winter temperatures in cold substages during the Karga interstadial were colder than those during the Sartan glacial event. The Late Pleistocene–Holocene climate history included several warm intervals when air temperatures were high enough to maintain the existence of low canopy tree patches in Kotelny Island. Mean January air temperatures in the early Holocene were only 1.0–1.5 °C lower than now. The early Holocene vegetation conditions were favorable for prolific growth of shrubs and fast peat accumulation.

Holocene, Late Pleistocene, ice complex, yedoma, winter paleotemperature, ice wedge, oxygen and hydrogen stable isotopes, radiocarbon age, Arctic islands

INTRODUCTION

The aim of this study is to investigate the oxygen and hydrogen isotope compositions of Late Pleistocene and Holocene ice wedges in Kotelny Island in the northeastern Russian Arctic during key climate events, with implications for winter air temperatures and climate conditions, including vegetation.

Kotelny Island was presumably discovered in 1773 by a merchant Ivan Lakhov while he was observing migrating herds of reindeer. The island is called Kotelny after the word *kotel* (Russian for *Kettle*) as the pioneers who explored the island left there a big copper kettle [*Ship History in Russia*, 2018]. E. Toll [1897] was the first geologist to visit the island and A. Lozhkin [1977] was the first to obtain ¹⁴C ages for its ice-rich permafrost (ice complex or *yedoma* deposits). V. Makeev *et al.* [1989] studied thick ice wedges in outcrops along the Balyktakh River, where they found many mammoth bones, and performed high-resolution radiocarbon dating of the ice complex deposits. In 1999 a group of German and Russian Scientists visited Kotelny Island and sampled two ice complex sections in its northern part near Cape Anisii and in the Khomurgannakh River mouth in the southwest [*Schirmeister et al.*, 2003, 2011]. Gravelly sand with ice wedges was sampled in the southern coast of the island, at 2.5–3.5 m above the sea level [*Dereviagin et al.*, 2007]. In 2012 N. Belova and a team from Moscow University [*Belova et al.*, 2015] studied two small ice complex outcrops in the southern part of the island.

Study area

Kotelny Island (74–76° N, 136–145° E) belongs to the Anjou group of islands in the New Siberian Archipelago between the Laptev and East Siberian seas. The island landscapes are mostly low Late Quaternary plains, ≤50 m asl, composed of ice-rich permafrost with tundra vegetation (Fig. 1), as well as flat or gently sloping lowlands (from 50 to 300 m asl), often with a rugged surface topography and with mountain Arctic desert vegetation.

Climate and vegetation

The island lies in the zone of Arctic climate, with a mean annual air temperature of –14.3 °C and a mean monthly July temperature of +2.9 °C. February is the coldest month, with a monthly air temperature mean of –29.7 °C. The lowest temperature (–49.5 °C) was recorded in the February of 2002 and the highest (+25.1 °C) in the July of 1991. Temperatures below –30 °C may occur from October to April. Mean daily temperatures become positive and negative on 13 June and 18 September, respectively [*Dobrowolska*, 2014; *Climate of Kotelny Island*, 2018].

According to geobotanic regional division, vegetation in the island belongs to the zone of shrub-moss Arctic deserts [*Gorodkov*, 1956]. The tundra vegetation on relatively elevated areas consists mainly of *Salix polaris* Wahlenb., *Alopecurus alpinus* Sm., *Saxifraga oppositifolia* L., *Saxifraga nivalis* L., *Papaver radicum* Rottb., *Dryas octopetala* L., *Cassiope*

tetragona (L.) D. Don, *Luzula confusa* Lindeb., *Ranunculus hyperboreus* Rottb., *Endocellion glaciale* (Ledeb.) J. Toman and the mosses *Ditrichum flexicaule* (Schwägr.) Hampe, *D. capillaceum* (Hedw.) Bruch et al. [Gorodkov, 1956].

Subfossil pollen spectra in Kotelny Island contain 22–44 % shrub pollen on average (willow, alder, and dwarf birch). The herb pollen taxonomy (mostly Poaceae, Polygonaceae, Caryophyllaceae, and Asteraceae) records the features of local phytocenoses. Many pollen spectra from the northern part of the island contain some single dominant component, often the spores of Bryales or *Selaginella sibirica*, which may reach 70–90 %. Such pollen spectra occur in ice complex sections and are interpreted as representative of polar deserts. The subfossil spectra have high percentages (20 to 90 %) of pollen and spores redeposited from Neogene sediments [Lozhkin, 1977, 2002].

Geocryology

The first evidence of geocryological conditions in the New Siberian Islands can be found in [Gorodkov, 1948]. The thaw season lasts no longer than 75 days, with thawing at a slow rate of 0.3–0.5 cm/day [Kachinskii, 2014] to depths from 10–28 cm in depressions between mounds to 48 cm on tops of thermokarst mounds (locally called *baydzherakh*).

The ice complex deposits occur at elevations of 15–30 m [Schirmeister et al., 2011]. They have thermokarst depressions and thermal erosion gullies on their tops and thermokarst mounds on the slopes. The Late Pleistocene and Holocene deposits comprise the stratigraphic units [Makeev et al., 1989] of (1) Dragotsennaya (Q_{III} dr) deposited mainly during the Kazantsevo and Zyryanka periods; (2) Balyktakh (Q_{III} bl) similar in volume to the Karga and a large part of the Sartan events; (3) Srednyaya (Q_{III-IV} sr), consisting of upper Late Pleistocene and lower Holocene deposits; and (4) Middle-Late Holocene Tugutakh (Q_{IV} tg). The total sediment thickness is within 50–60 m [Makeev et al., 1989].

Structure of ice wedges and sampling

Syncryogenic ice complex deposits were studied previously [Makeev et al., 1989] in the southern coast of Kotelny island, in the Balyktakh River valley, and in the northwestern island part (Fig. 2, a).

Sampling site M-1 (Fig. 3, a) is located in the southern coast near the Karga River mouth (Fig. 1), where layered permafrost composed of bluish-grayish silt with inclusions of brown peat rolls or less often fine pebbles, as well as thin or thick ice lenses, is exposed in the bluff. A peat lens occurs about 5 m above the water table and silt encloses an ice wedge, ~3.5 m wide on top and ~5 m high. Silt and clay silt layers warp up at the contact with the ice. The ice is columnar, with alternated turbid and transparent layers.

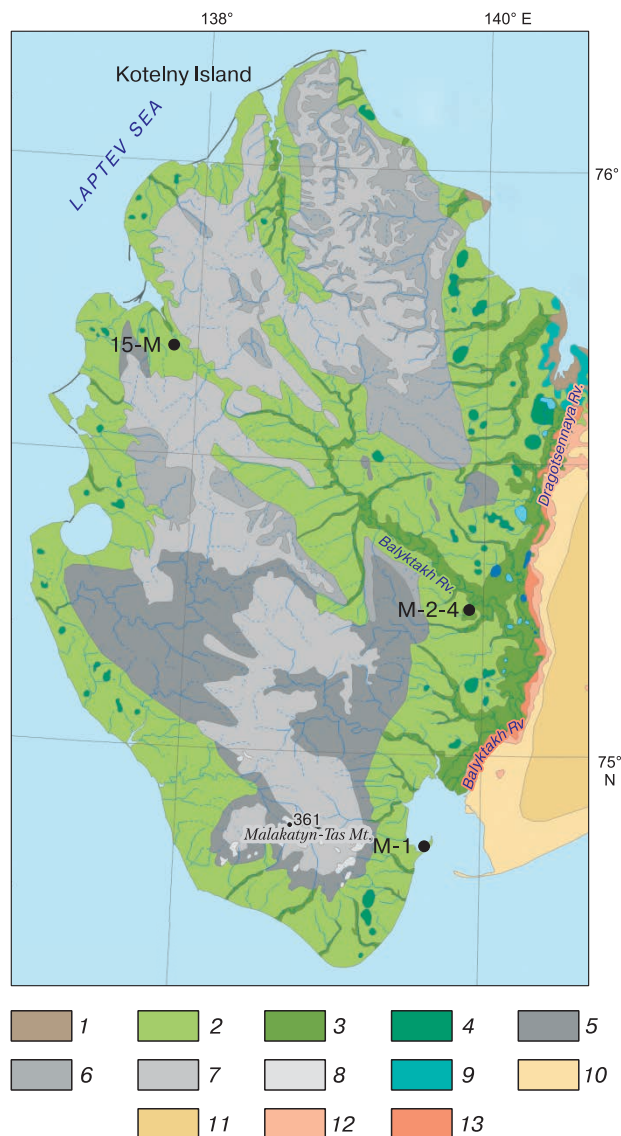


Fig. 1. Location of reference sections with ice wedges in the landscape map of Kotelny Island, simplified after [Troshko, 2018].

1 – tidal drain areas; 2 – lowland plains (within 50 m asl) composed of moderately eroded ice complex deposits with thermokarst and tundra vegetation; 3 – river valleys with palustrine vegetation; 4 – bottoms and sides of thermokarst depressions (alases); 5 – flat and gently sloping low plains (50–100 m asl); plateau-like elevated plains (100–300 m asl) with Arctic desert vegetation; 6 – heavily eroded undulated surfaces; 7 – weakly eroded flat and low-angle surfaces; 8 – rounded-top ridges, higher than 300 m asl, almost devoid of vegetation; 9 – coastal plain, within 8 m high, with thermokarst erosion and palustrine vegetation; 10 – marine terrace I, within 10 m high, with Arctic desert vegetation and Aeolian micro-scale surface topography, within 3 m; 11 – marine terrace I, <10 m high, with Arctic desert vegetation and Aeolian micro-scale surface topography, within 3–10 m; 12 – marine terrace II, 10–25 m high, mainly eroded, with Arctic desert vegetation; 13 – eroded marine terrace II, 10–25 m high, mainly with tundra vegetation. M-1, M-2-4, 15-M are sampling sites.

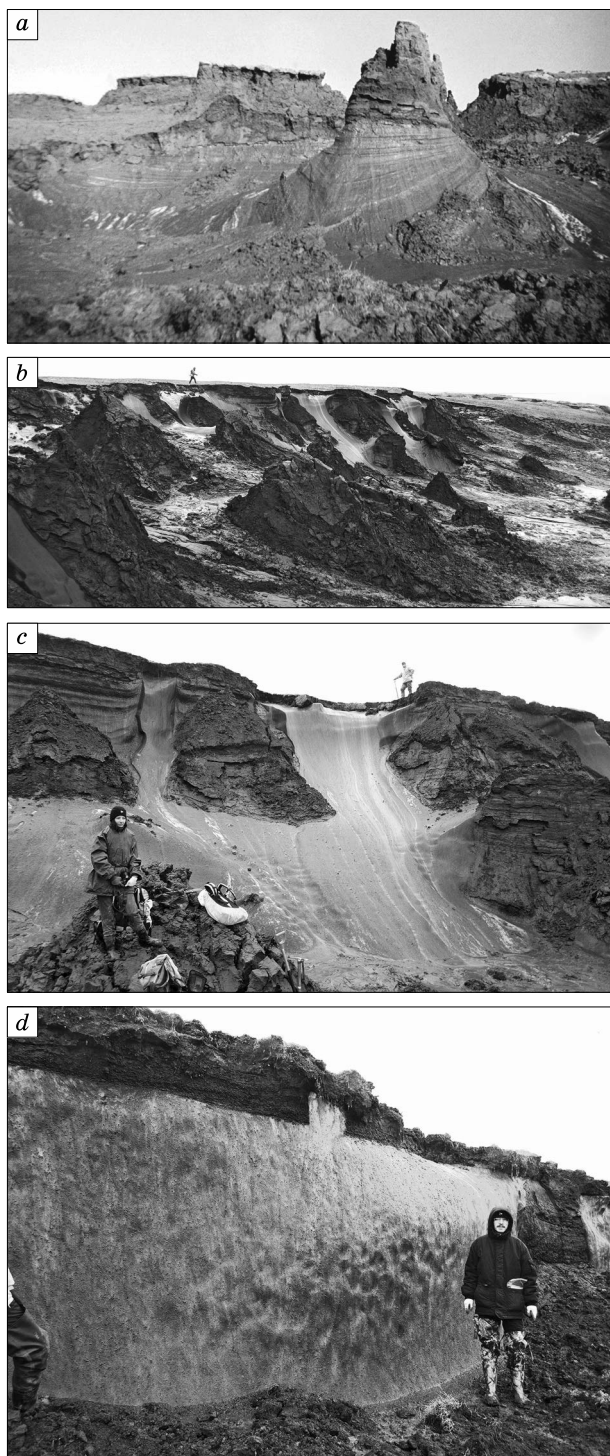


Fig. 2. Ice complex deposits and Late Pleistocene ice wedges.

Photographs are by V. Makeev (a), and courtesy N. Belova (b–d).

Ten ice samples were collected at every 30 cm for isotope analysis (Fig. 3, a). Peat from the peat lens was sampled for radiocarbon dating.

Sites M-2–4 (Fig. 3, b) are located in the Balyktakh middle reaches, in the right side of the valley (Fig. 1). Horizontally layered silt with lenses of detrital peat and ice wedges crop out discontinuously in the bluff, over a distance of >50 m. Most of exposed ice wedges are 3.0–3.5 m wide and up to 4 m high. Ice wedge 4, at the top of a thermokarst mound, is about 1 m wide and 1.5 m high. Ice is columnar in all wedges. The sediments are cut by 2.5 m of younger layered dark-gray alluvial silt with intercalations of detrital peat. Samples for stable isotopes were taken from ice wedges 2–4, as well as from ice lenses that host ice wedges 2 and 3 (wedge 2 may enclose Holocene ice). Peat was sampled for radiocarbon analysis.

Site 15-M is located in the northwestern part of the island where A. Maslakov sampled Holocene ice wedges in 2015 (Fig. 4, a, b), on a gently sloping surface (24–38 m asl). Permafrost at the site is composed of gray or less often light-brown clay silt, locally with abundant debris, and has massive or sometimes reticulate cryostructures. Clay silt encloses lenses and nests of ice-bonded black or dark brown peat with plant rootlets. A 5–10 cm thick peat layer crops out near the top of the clay silt layer. The ice wedge has sharp and smooth sides and top. The 1 cm thick top layer of transparent ice with up to 5 mm vertical elongated air bubbles lies 0.4 m below the ground surface. The wedge consists of columnar ice with vertically alternated light and dark turbid and transparent layers that enclose abundant 0.5 to 3.0 mm air bubbles. Ice was sampled for stable isotope analysis at every 0.2 m along a horizontal profile, 0.6 m below the surface (Fig. 4, c).

Methods

Holocene organic matter from the ice complex deposits was dated by the radiocarbon method (^{14}C) at the Institute of Material Culture History, St. Petersburg (laboratory ID of samples LE). Stable isotopes (oxygen and hydrogen) were measured in the ice wedge at site 15-M sampled in 2015, at the Isotope Laboratory of the Faculty of Geography of Moscow University. The analysis was performed on a *Finnigan Delta-V Plus* mass spectrometer with a standard gas-bench option and the results were calibrated against international (V-SMOW and SLAP) and laboratory standards, with internal 1σ errors of $\pm 0.6\%$ for $\delta^2\text{H}$ and $\pm 0.1\%$ for $\delta^{18}\text{O}$. Oxygen isotope ratios in ice wedges were determined on a *Finnigan Delta-E* mass spectrometer at the Isotope Laboratory of the Institute of Geology of Estonia.

RESULTS

Radiocarbon dating of permafrost

Holocene syncryogenic sediments in the northwestern part of Kotelny Island (Fig. 4, c) have ^{14}C ages of 8660 ± 35 yr BP for peat sampled at a depth of 0.7 m 0.5 m left of the ice wedge (LE-11256) and

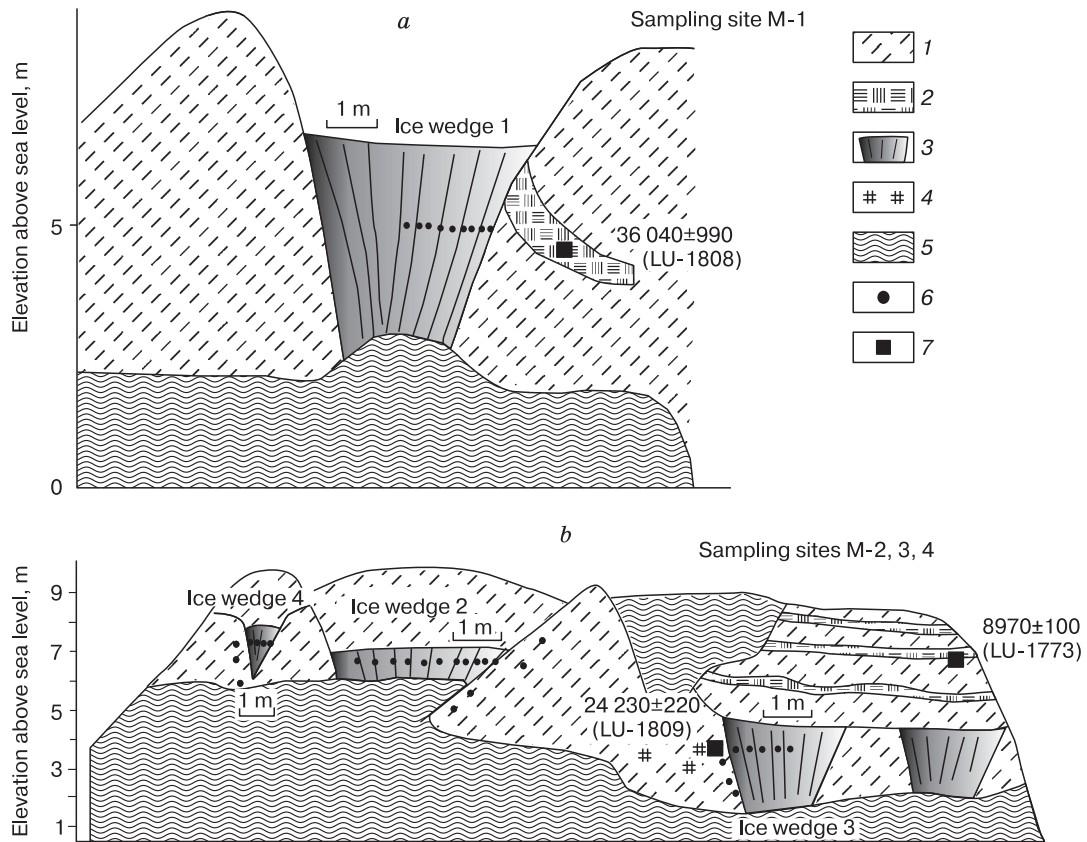


Fig. 3. Radiocarbon ages and sampling sites for isotope analysis in Late Pleistocene ice complex deposits with ice wedges.

Ice wedges in the southern coast of Kotelny Island (a) and in the Balyktakh valley (b). 1 – silt; 2 – peat; 3 – ice wedges; 4 – peat patches; 5 – mud slides and talus; 6 – sampling sites of ice wedges for isotope analysis; 7 – sampling sites for AMS ¹⁴C dating and ages.

9310 ± 66 yr BP for that from a depth of 1.4 m, sampled 4 m left of the wedge (LE-11258).

The available ages of Late Pleistocene syn-cryogenic ice complex deposits are, respectively, 24 230 ± 220 yr BP (LU-1809) and 10 000 yr BP (LU-1773) for autochthonous peat below and above an ice wedge in the Balyktakh valley (Fig. 3, b) [Makkeev et al., 1989, 2003], and 36 040 ± 990 yr BP for a peat layer (LU-1808) bent toward an ice wedge in the southern coast (Fig. 3, a).

Oxygen and hydrogen isotope compositions of ice wedges

The obtained stable isotope ratios for Late Pleistocene ice wedges in Kotelny Island have more negative values than their Holocene counterparts.

The $\delta^{18}\text{O}$ values range in Late Pleistocene ice wedge 3 (Fig. 3) is from -30.0 to -27.4 ‰ (-28.5 ‰ on average), and that in adjacent lenses of segregated ice is -27.4 to -24.6 ‰ $\delta^{18}\text{O}$ values (-25.5 ‰ on average). Two ice wedges (2 and 4) located slightly higher stratigraphically, near the unit top, have the respective ranges of -26.2 to -22.9 ‰ and -27.1 to

-24.9 ‰ $\delta^{18}\text{O}$ values (-25.9 ‰ on average); ice wedge 2 encloses apparently Holocene ice with -22.9 to -23.9 ‰ $\delta^{18}\text{O}$ values.

The $\delta^{18}\text{O}$ and $\delta^2\text{H}$ values in the Holocene ice wedge from the northwestern island part are, respectively, -23.14 to -21.64 ‰ (average -22.5 ‰) and -174.1 to -163.1 ‰ (average -169.3 ‰); deuterium excess (d_{exc}) is from 6.9 to 12.8 ‰, average 10.4 ‰ (Tables 1, 2).

The Holocene ice wedge composition plots close to the global meteoric water line (GMWL) in the $\delta^{18}\text{O}$ – $\delta^2\text{H}$ diagram (Fig. 5). This indicates the meteoric origin of water and equilibrium isotope fractionation during the formation of the water and the respective ice wedges.

A linearly approximated $\delta^{18}\text{O}$ – $\delta^2\text{H}$ diagram shows a slope of 6.7 and an intercept of -18.7 (equation $y = 6.7x - 18.7$; approximation reliability $R^2 = 0.7$), with narrow $\delta^{18}\text{O}$ and $\delta^2\text{H}$ ranges (1.5 and 11 ‰, respectively). The proximity of the Holocene ice wedge $\delta^{18}\text{O}$ values to GMWL allows using them for paleotemperature reconstructions. The $\delta^{18}\text{O}$ and $\delta^2\text{H}$ values obtained for the Holocene ice wedge agree

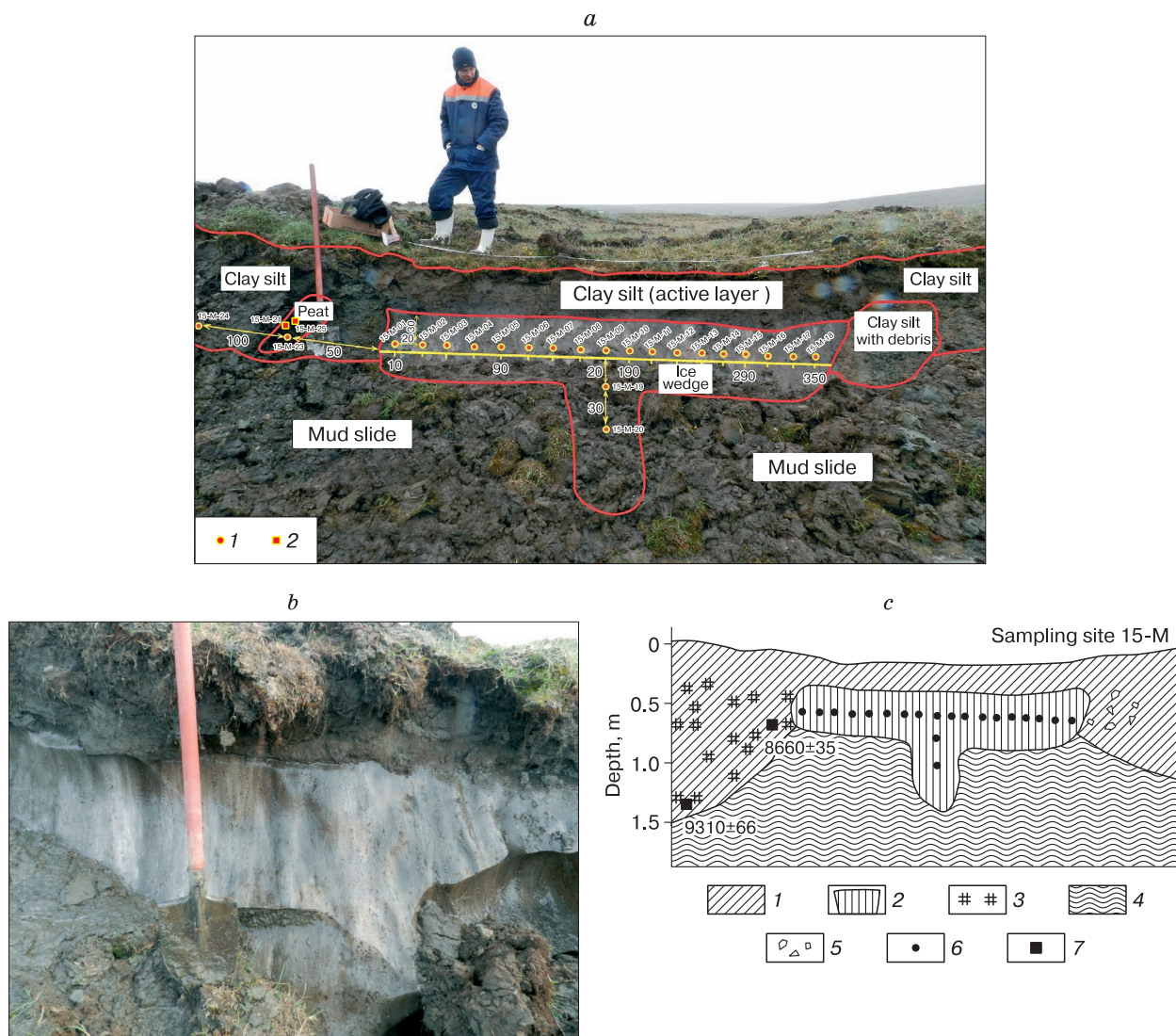


Fig. 4. Outcrop of Holocene ice wedges in the northwestern coast of Kotelny Island (a, b) and sampling sites for radiocarbon dating (c).

1 – clay silt; 2 – ice wedge; 3 – peat lenses and nests; 4 – mud slides and talus; 5 – debris; 6 – sampling sites of ice wedges for isotope analysis; 7 – ¹⁴C ages. Photograph by A. Maslakov.

with those for the ice wedge top reported by *Belova et al.* [2015] (Fig. 2, b–d): –29 to –24 ‰ in the lower part (depth 2.5 m) and –25 to –20 ‰ in the upper part. According to *Belova et al.* [2015], Late Pleistocene wedges may enclose Holocene ice wedges in their upper part (Fig. 2, d), judging by $\delta^{18}\text{O}$ values uncommon for Late Pleistocene ice and by the presence of a younger and narrower ice wedge inside the older one (a very rare cryological phenomenon). Such relations of Late Pleistocene and Holocene ice wedges were reported from the Bykov Peninsula [Vasil'chuk, 1988], as well as from the Oygos Yar coast of the Dmitry Laptev strait and Bolshoy Lyakhovsky Island, where

air bubble methane from the upper wedge part shows a Holocene age [Morizumi et al., 1995].

Late Pleistocene and Holocene climate and environment

The available ages of permafrost in Kotelny Island vary from 55 Kyr BP in its northwestern part and in the Khomurgannakh River mouth (Fig. 1) to 27.8–11.0 Kyr BP in the northern part, at Cape Anisii [Schirrmester et al., 2011], and to 11.9 Kyr BP in the Balytakh River valley [Pavlova et al., 2009]. The ages of ice wedges in the southern island coast have been constrained by two AMS ¹⁴C dates for plant detritus

Table 1. $\delta^{18}\text{O}$, $\delta^2\text{H}$ and d_{exc} in Holocene ice wedges in northwestern part of Kotelny Island (site 15-M)

Sample ID	Depth, m	Distance from left margin of ice wedge, m	$\delta^{18}\text{O}$, ‰	$\delta^2\text{H}$, ‰	d_{exc} , ‰
15-M-02	0.57	0.3	-22.64	-174.1	7.02
15-M-03	0.57	0.5	-21.64	-166.2	6.92
15-M-04	0.57	0.7	-22.12	-164.8	12.16
15-M-05	0.57	0.9	-22.80	-171.4	11.0
15-M-06	0.57	1.1	-22.76	-169.3	12.78
15-M-07	0.57	1.3	-22.98	-172.4	11.44
15-M-08	0.57	1.5	-22.25	-166.2	11.8
15-M-09	0.57	1.7	-21.95	-165.2	10.4
15-M-10	0.57	1.9	-22.85	-173.8	9.0
15-M-11	0.57	2.1	-22.69	-169.6	11.92
15-M-12	0.57	2.3	-23.14	-173.4	11.72
15-M-13	0.57	2.5	-21.81	-163.1	11.38
15-M-14	0.57	2.7	-22.64	-168.3	12.82
15-M-15	0.57	2.9	-22.64	-170.0	11.12
15-M-16	0.57	3.1	-22.71	-172.4	9.28
15-M-17	0.57	3.3	-22.18	-167.8	9.64
15-M-18	0.57	3.5	-22.35	-170.6	8.2
15-M-19	0.77	1.7	-22.30	-169.2	9.2

Table 2. $\delta^{18}\text{O}$ (‰ relative to V-SMOW) in Late Pleistocene ice wedges and segregated ice in Balyktakh River valley and in Sopochnaya Karga Peninsula

Sample ID	Ice type	Elevation*, m	$\delta^{18}\text{O}$, ‰	Sample ID	Ice type	Elevation*, m	$\delta^{18}\text{O}$, ‰
<i>Balyktakh Valley</i>							
M-2/1	Ice wedge	6.5 (0.3)	-22.9	M-4/1	Segreg.	6.0	-25.6
M-2/2	Ice wedge	6.5 (0.7)	-23.3	M-4/2	Segreg.	6.5	-24.2
M-2/3	Ice wedge	6.5 (1.1)	-23.9	M-4/3	Segreg.	6.8	-26.4
M-2/4	Ice wedge	6.5 (1.5)	-26.3	M-3/1	Ice wedge	3.8 (0.2)	-29.7
M-2/5	Ice wedge	6.5 (1.8)	-24.8	M-3/2	Ice wedge	3.8 (0.6)	-30.0
M-2/6	Ice wedge	6.5 (2.1)	-24.8	M-3/4	Ice wedge	3.8 (1.0)	-28.2
M-2/7	Ice wedge	6.5 (2.5)	-25.1	M-3/5	Ice wedge	3.8 (1.5)	-27.4
M-2/8	Ice wedge	6.5 (2.8)	-24.5	M-3/6	Ice wedge	3.8 (1.9)	-27.4
M-2/9	Ice wedge	6.5 (3.1)	-24.9	M-3/7(1)	Segreg.	2.0	-27.4
M-2/10	Ice wedge	6.5 (4.0)	-26.2	M-3/8(2)	Segreg.	2.5	-24.6
M-2/11	Ice wedge	6.5 (4.5)	-24.0	M-3/9(3)	Segreg.	3.3	-24.6
M-2/12	Segreg.	5.0	-26.7	M-4/1	Ice wedge	6.8 (0.2)	-26.1
M-2/13	Segreg.	5.5	-27.7	M-4/2	Ice wedge	6.8 (0.5)	-25.7
M-2/14	Segreg.	6.4	-28.6	M-4/3	Ice wedge	6.8 (0.8)	-24.9
M-2/15	Segreg.	7.3	-29.9	M-4/4	Ice wedge	6.8 (1.2)	-27.1
<i>Sopochnaya Karga Peninsula, coast of Sannikov Strait</i>							
M-1/1	Ice wedge	+5 (0.1)	-30.1	M-1/5	Ice wedge	+5 (1.3)	-30.6
M-1/2	Ice wedge	+5 (0.4)	-30.5	M-1/8	Ice wedge	+5 (1.9)	-30.5
M-1/3	Ice wedge	+5 (0.7)	-30.3	M-1/8	Ice wedge	+5 (2.0)	-30.2
M-1/4	Ice wedge	+5 (1.0)	-29.9	M-1/9	Ice wedge	+5 (2.3)	-30.4

* Elevations above river level (from right wedge side) for Balyktakh Valley and above sea level for Sannikov Strait.

and moss: 45 960 + 2460/ - 1880 yr BP (KIA-25741) and 52 790 + 4110/ - 2710 yr BP (KIA-25743) [Meyer et al., 2002; Dereviagin et al., 2007]. The oldest reliable AMS ^{14}C ages of plant detritus and peat samples from the Khomurgannakh mouth [Schir-

rmeister et al., 2011] record the onset of deposition about 55 Kyr BP (Fig. 6). As shown by published evidence [Makeev et al., 1989, 2003; Schirrmeyer et al., 2003, 2011; Pavlova et al., 2009; Vasil'chuk et al., 2016, 2018] and this study, ice wedges formed rapidly

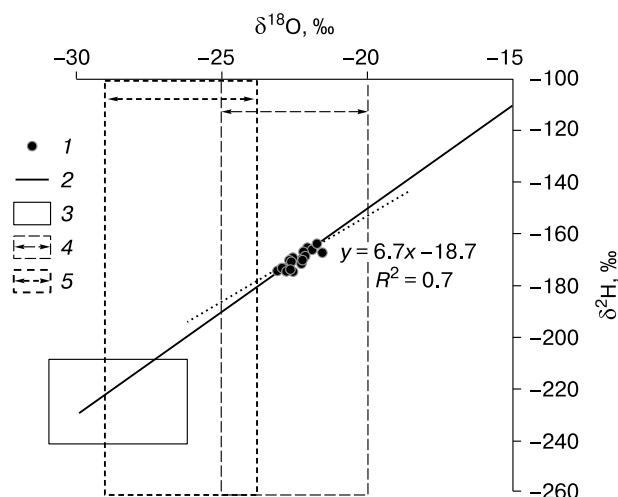


Fig. 5. $\delta^2\text{H}$ – $\delta^{18}\text{O}$ diagram (dotted line) for Holocene ice wedges in the northwestern coast of Kotelny Island (site 15-M) and $\delta^2\text{H}$ – $\delta^{18}\text{O}$ diagram for Late Pleistocene ice wedges.

1 – $\delta^{18}\text{O}$ and $\delta^2\text{H}$ values in ice; 2 – global meteoric water line (GMWL); 3 – $\delta^{18}\text{O}$ and $\delta^2\text{H}$ ranges in Late Pleistocene ice wedges after [Dereviagin et al., 2007]; 4 – $\delta^{18}\text{O}$ range in upper part of an ice wedge after [Belova et al., 2015]; 5 – $\delta^{18}\text{O}$ range in lower part of an ice wedge after [Belova et al., 2015].

during the 50–45, 35–25, 22–12 and 9–2 Kyr BP cold spells.

Samples from northwestern Kotelny Island have AMS ^{14}C ages of $29\,750 \pm 1100$ yr (MAG-144) and $28\,220 \pm 1000$ yr BP (MAG-174) for the middle and top parts of the peat layer, respectively [Lozhkin, 1977]. Pollen spectra of peat samples record mosaic patterns of taxonomically diverse plant communities with predominant grass pollen (53 %), among which abundant Poaceae (50 %), moderate percentages of Cyperaceae (17 %), *Artemisia* (18 %), and minor Liliaceae (3 %), Polygonaceae (2 %), Caryophyllaceae (13 %), Ranunculaceae (2 %), Fabaceae, Ericales, Compositae etc., as well as dwarf birch, willow, and alder (14 % in total), Siberian dwarf pine, and spruce. The presence of lily-flowered species and willow indicates favorable conditions for pollen preservation and, hence, rather rapid transition to the perennially frozen state. Carpological analysis of peat (by V. Nikitin) reveals *Eriophorum* sp., *Carex* sp. and *C. cf. pauciflora* Lightf., the species occurring much farther to the south in the Aldan and Upper Vilyui catchments, as well as three species of moss spread over a large area from the forest zone to the Arctic. Thus, the pollen spectra of the 34 to 29 cal. Kyr BP time span belong to typical tundra-steppe vegetation with predominant Poaceae and *Artemisia* [Lozhkin, 1977].

The ice complex (yedoma) with syngenetic ice wedges on the right side of the Balyktakh River ($75^{\circ}15' \text{ N}$, $139^{\circ}54' \text{ E}$) forms marine terrace II and is

covered with peat-bearing palustrine deposits. Previous AMS ^{14}C dating of the section gave nine ages from $20\,840 \pm 100$ yr BP (Beta-190097) to 9090 ± 40 yr BP (LE-6368) [Pavlova et al., 2009]. Well preserved wood samples from a thermokarst mound at $75^{\circ}21'32'' \text{ N}$, $139^{\circ}15'05'' \text{ E}$ showed an age of $40\,200 \pm 2400$ yr BP (IM-55) (sampled by Protopyov [Galanin et al., 2015]), and the oldest dates for Kotelny Island are bracketed between 47 641 and 39 528 cal. yr BP (Fig. 6). More ages obtained for plant and bone fossils from the Khomurgannakh River mouth and the Balyktakh valley give a range of 40 400–36 100 cal. yr BP (Fig. 6). As Makeev et al. [1989] concluded from pollen spectra, forest patches existed along river valleys during the Balyktakh deposition (>54–28 Kyr BP) while steppe and tundra-steppe landscapes still predominated on watersheds.

Plant remnants, wood, and bones from ice complex sections in the northwestern coast of Kotelny Island, as well as in the Balyktakh valley and Cape Anisii, have AMS ^{14}C ages in the range 36 to 22 cal. Kyr BP. A. Protopyov found larch remnants in a thermokarst mound at $75^{\circ}23'17'' \text{ N}$, $139^{\circ}18'42'' \text{ E}$, which presumably occurred *in situ* about 530 km north of the present northern larch tree line. Peat from that site also stores needles and bark pieces of larch and birch remnants. High-resolution pollen spectra of 36 583–35 469 cal. yr BP sediments that host a larch trunk (Fig. 6) record mosaic meadow-steppe vegetation with forest patches [van Geel et al., 2017]. Both samples contain *Larix* pollen, which provides solid evidence for the presence of *Larix* in the respective plant communities, as its pollen is fragile and hardly can travel long distances [Vasil'chuk and Vasil'chuk, 2018]. Larch also grew earlier in the area, judging by 47 641–39 528 cal. yr ^{14}C ages of wood samples [Galanin et al., 2015].

There are no AMS ^{14}C ages of plant remnants available for the 22.7 to 17.0 cal. Kyr BP interval, but Sulerzhitsky and Romanenko [1997] obtained 22.4 to 20.9 cal. Kyr BP radiocarbon ages for collagen from mammoth teeth and horse bones (Fig. 6). We infer that the vegetation of the island between 20 and 17 cal. Kyr BP was insufficient to feed large mammals, which migrated to areas with more favorable conditions; after that period, the vegetation recovered. Plant and bone remnants from the Balyktakh valley bracket the age of their host sediments between 16.9 and 10.9 cal. Kyr BP. Pollen spectra [Makeev et al., 2003] record predominant xerophytes (mostly *Artemisia*) in the 15.4–12.5 cal. Kyr BP interval and marked vegetation change at 12.5–12.2 cal. Kyr BP, with high percentages of shrub pollen (45 %): *Betula* sect. *Fruticosa* and *Betula* sect. *Nanae*; *Alnus fruticosa*, and *Salix* sp. The latest Pleistocene pollen spectra (12.2–10.0 cal. Kyr BP) contain within 20 % of tree and shrub pollen, and abundant xerophytes [Makeev et al., 2003].

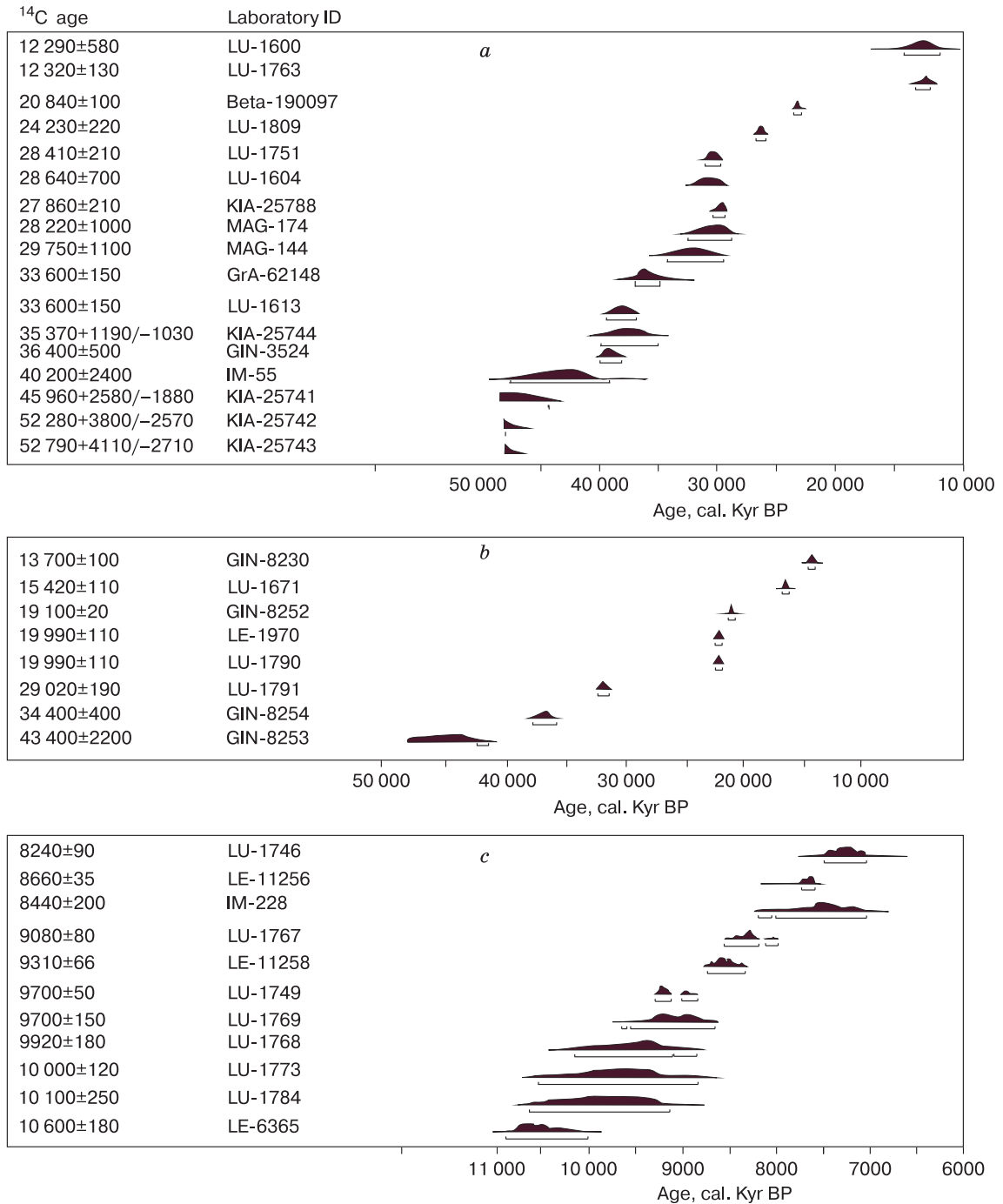


Fig. 6. Calendar age of ice complex deposits that enclose ice wedges in Kotelny Island.

a: Late Pleistocene ages of plant detritus and wood; *b*: Late Pleistocene ages of bone fossils; *c*: Holocene ages of plant detritus. ¹⁴C ages were calibrated using the *Oxcal 4.2* software [Bronk Ramsey, 2009] based on *IntCal13* calibration database [Reimer et al., 2013], according to radiocarbon dating [Lozhkin, 1977; Makeev et al., 1989; Sulerzhitsky and Romanenko, 1997; Pavlova et al., 2009; Schirmermeister et al., 2011; Galanin et al., 2015; van Geel et al., 2017; this study].

Radiocarbon ages of Holocene peatlands in a range of 10 to 7 cal. Kyr BP (Fig. 6) were obtained for samples from the northwestern island coast: the Khomurgannakh River mouth and the Dragotsenna-

ya and Balyktakh valleys. The respective pollen spectra do not show dramatic changes and are generally similar to the present subfossil spectra [Makeev et al., 1989], except for high percentages of dwarf birch, al-

der, and willow in the 10–9 cal. Kyr BP interval. It was a time of active thermokarst processes that produced thaw lakes (which later dried out to form alas depressions) and maintained peat deposition at 0.4–0.5 cm/yr; tall shrubs appeared in river valleys. As reported by D. Ponomareva [Makeev *et al.*, 2003], the spectra for the 8–7 cal. Kyr BP interval show high percentages of tree and shrub pollen (up to 40 %), mainly *Betula* sect. *Fruticosa*, *B.* sect. *Nanae*, and *Salix*, while peat contains detritus of tall shrubs. Shrub pollen reaches especially high percentages at 7.5–7.0 cal. Kyr BP, which supports the hypothesis of Gorodkov [1956] that thick peatlands formed in the island in the earliest Holocene. Peat deposition in the island continued also later. Samples from the base and top of a large peatland from the lowermost section of terrace I of the Balyktakh River have ages of 5460 ± 100 yr BP (LE-6433) and 3040 ± 100 yr BP (LE-6429), respectively [Anisimov, 2010]. A series of dates for samples from the terrace top reported by Anisimov [2010] constrains the onset of river incision, which changed the base level of erosion, between 3870 ± 90 yr BP (LE-6408) and 3480 ± 100 yr BP (LE-6422). Analysis of plant remnants revealed periodic slight changes in humidity that repeated every tens to hundreds of years [Anisimov, 2010]. A 1.1 m thick lens of dark brown poorly degraded layered sedge-grass peat with up to 2 cm thick lens-like ice layers showed ages of 1530 ± 80 yr BP (LU-1473) from a depth of 0.3 m and 6250 ± 390 yr BP (LU-1470) from 1.0–1.1 m below the peat top [Makeev *et al.*, 1989].

As shown by paleotemperature reconstructions from various analytical data [Vasil'chuk A.C., 2003; Kienast *et al.*, 2011; Zimmermann *et al.*, 2017], the Late Pleistocene history of Arctic Northeastern Siberia included warm spells with rather high summer temperatures and long vegetation periods, which maintained patch growth of trees and tall shrubs far beyond the Arctic Circle. Specifically, they were the spells between 48–35 Kyr BP in Kotelny Island (according to plant detritus ages) and between 48 and 38 Kyr BP in Bolshoy Lyakhovskiy Island [Wetterich *et al.*, 2014]. Ice complex deposition in Kotelny Island lasted from no later than 55 Kyr BP (in the northwestern part of the island and in the Khomurgannakh mouth) [Schirrmeyer *et al.*, 2011] to 11–10 Kyr BP [Makeev *et al.*, 2003].

Ice complex deposits were studied in five outcrops during the joint Russian-German trip to the New Siberian Islands in 2002 [Schirrmeyer *et al.*, 2002]. L. Schirrmeyer and T. Kuznetsova, with colleagues, found more than 30 mammoth and horse bones *in situ* in Cape Anisii [Schirrmeyer *et al.*, 2003]. Especially important was the finding of two Holocene (3000 ± 45 and 2800 ± 120 yr BP) horse bones reported by Kuznetsova [Schirrmeyer *et al.*, 2003]

which indicate that the local landscapes of that time were productive enough to provide food for horse populations. In the summer of 2018, A. Protopopov and his colleagues found remnants of an adult dwarf mammoth (a fragment of a front leg and a shoulder blade) in the tidal zone of Kotelny Island [Remnants of a Small Mammoth Discovered in Kotelny Island, 2018]. Analysis and dating of these samples will shed light on the Late Pleistocene–Holocene history of mammoths.

The first palynological analysis of ground ice in Kotelny Island, based on 664 pollen grains from a >20 kg ice sample, showed spectra with 4 % tree pollen, 80 % grass and shrub pollen, and 16 % spores (sampling by B. Gorodkov; analysis by R. Fedorova) [Grichuk and Fedorova, 1956]. Some pollen was redeposited from pre-Quaternary rocks. The tree pollen mainly belongs to *Pinus sibirica* vs. *P. sylvestris* and some *Picea*, *Betula* and *Alnus*; grasses and shrubs comprise 52 % *Artemisia* and 35 % Poaceae. The spectra contain immature trisulcate pollen unidentifiable to family, as well as pollen of Chenopodiaceae, Caryophyllaceae, and Ericaceae, but lack willow, sedge, and larch, although ice ensures good preservation conditions [Grichuk and Fedorova, 1956]. B. Gorodkov interpreted the sample as massive ice [Grichuk and Fedorova, 1956] but it rather appears to be a Late Pleistocene ice wedge with a generalized record of spring pollen rain.

Oxygen and hydrogen isotope compositions of Late Pleistocene ice wedges

The $\delta^{18}\text{O}$ values we revealed in Late Pleistocene ice wedges from the Balyktakh valley in Kotelny Island (from -30.0 to -27.4 ‰ and -22.9 to -27.1 ‰ in lower and upper wedges, respectively) are 3–5 ‰ less negative from 23 to 10 Kyr BP than in earlier times. These results are consistent with the published evidence cited above.

Similar $\delta^{18}\text{O}$ variations were obtained for other Late Pleistocene ice wedges from the New Siberian Islands. They are -32.5 to -28.5 ‰ $\delta^{18}\text{O}$ near the Zimovye River and -26.5 to -21.0 ‰ $\delta^{18}\text{O}$ (-24.5 ‰ on average) in alas depressions in Bolshoy Lyakhovskiy Island, which are more depleted than the average $\delta^{18}\text{O}$ value for modern ice wedges from the Zimovye floodplain (-20.4 ‰) [Meyer *et al.*, 2002; Wetterich *et al.*, 2014]; from -28.65 to -27.85 ‰ (-28.5 ‰ on average) and -22.02 to -19.97 ‰ for Late Pleistocene and Holocene samples, respectively, in Zhokhov Island [Pavlova *et al.*, 2015]; average values of -31 ‰ $\delta^{18}\text{O}$ and -240 ‰ $\delta^2\text{H}$ in ice complex samples from the coast and less negative values in Holocene (11.5–3.6 cal. Kyr BP) ice wedges of a thermokarst depression at the Oygos Yar site, which enclose a -9.3 cal. Kyr BP peat layer: -25 to -26 ‰ $\delta^{18}\text{O}$ and -190 to -200 ‰ $\delta^2\text{H}$ [Opel *et al.*, 2017].

The oldest ages 45 960 + 2460/ – 1880 yr BP (KIA-25741) and 52 790 + 4110/ – 2710 yr BP (KIA-25743) were obtained for plant detritus and moss from gravelly sands in the southern coast of Kotelny Island. These sediments enclose ice wedges with rounded heads (Fig. 7) [Schirrmeyer *et al.*, 2011], which have –31.0 to –26.2 ‰ $\delta^{18}\text{O}$ (–29.5 ‰ on average) and –240.9 to –208.4 ‰ $\delta^2\text{H}$ (–229.9 ‰ on average), with d_{exc} from 1.5 to 8.0 ‰ (an average of 5.9 ‰) [Dereviagin *et al.*, 2007]. The Holocene ice wedges show generally higher d_{exc} values (an average of 10.4 ‰) than those reported by Dereviagin *et al.* [2007]. This misfit may result from variations caused by the Atlantic Ocean and distant air transport effects on snow and atmospheric precipitation in Kotelny Island in the Holocene.

Late Pleistocene and Holocene mean January and mean winter air temperatures in Kotelny Island

The oxygen isotope composition of ice wedges has implications for air temperatures during their formation. Mean winter (t_{mw}) and mean January (t_{j}) air temperatures in Kotelny Island can be found using the t – $\delta^{18}\text{O}_{\text{iw}}$ relationships [Vasil'chuk, 1991]:

$$t_{\text{mw}}^{\circ} = \delta^{18}\text{O}_{\text{iw}} (\pm 2^{\circ}\text{C}); t_{\text{j}}^{\circ} = 1.5\delta^{18}\text{O}_{\text{iw}} (\pm 3^{\circ}\text{C}).$$

These equations originally derived for recent ice veinlets in the present permafrost of northern Russia approximate well the data on such ice wedges in the Arctic islands (Table 3).

The $\delta^{18}\text{O}$ variations exceed 6 ‰ (from –30.6 to –24.0 ‰) in Late Pleistocene syngenetic ice wedges in Kotelny Island but are minor (within 1.5 ‰: –23.1 to –21.6 ‰) in their Holocene counterparts. The inferred mean January air temperatures were 5–8 °C colder and more variable (with a difference of 10–12 °C) in the Late Pleistocene but relatively stable (within 2 °C) in the Holocene; the respective Late

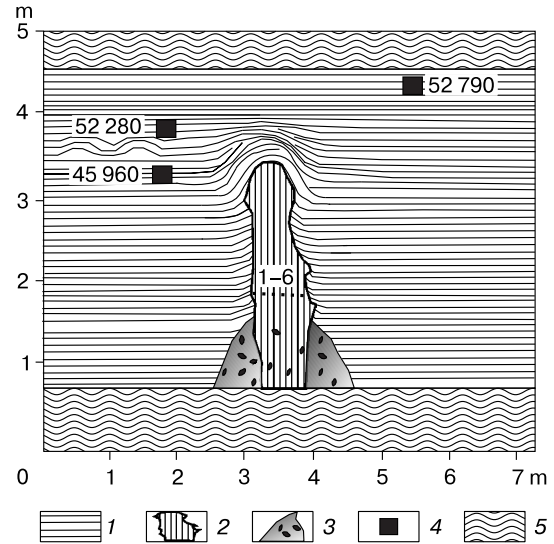


Fig. 7. Late Pleistocene ice wedges in the southern coast of Kotelny Island sampled for isotope analysis [Schirrmeyer *et al.*, 2003, 2011; Dereviagin *et al.*, 2007].

1 – ice complex deposits; 2 – buried syngenetic ice wedge (1–6 are sampling sites); 3 – sand with gravel; 4 – sampling sites for radiocarbon dating and ages in yr BP; 5 – mud slides.

Pleistocene mean winter air temperatures were 3–5 °C lower than the Holocene values.

Through the Late Pleistocene and Holocene history, the air temperatures and geocryological parameters inferred from $\delta^{18}\text{O}$ in syngenetic ice wedges in Kotelny Island were either more or less similar to those in other East Arctic islands (Table 4); this dissimilarity is interesting but not quite clear. The ice wedges of Kotelny and Ayon islands had similar oxygen isotope compositions between 35 and 25 Kyr BP and from 9 to 2 Kyr BP but $\delta^{18}\text{O}$ values in the Kotelny ice wedges were less negative than their Ayon

Table 3. $\delta^{18}\text{O}$ values in modern incipient syngenetic ice wedges in islands of Russian East Arctic, modified and complemented after [Vasil'chuk, 1992]

Location	Coordinates	$\delta^{18}\text{O}$, ‰	Σt_{w}	t_{mw}	t_{j}	t_{s}
Henrietta Island	77°06' N, 156°30' E	–15.3	–5330	–17	–27	–12
Zhokhov Island	76°09' N, 152°43' E	–20.0	–5363	–18	–29	–13
Kotelny Island	75°27' N, 140°50' E	–18.1	–5408	–19	–29	–14
Bunge Land*	75°24' N, 141°16' E	–17.6	–5989	–21	–28	–14
Maly Lyakhovsky Island	74°07' N, 140°40' E	–18.0	–5408	–20	–31	–14
Bolshoy Lyakhovsky Island*	74°07' N, 140°40' E	–20.4	–5400	–20	–31	–14
New Siberia Island	75°03' N, 148°28' E	–18.0	–5500	–20	–30	–14
Chetyrekhtolbovoy Island	70°47' N, 161°36' E	–20.0	–5143	–19	–30	–13
Ayon Island	69°47' N, 168°39' E	–21.0	–5047	–20	–29	–12

Note. Σt_{w} is the sum of winter air temperatures, °C·day (annual freezing index); t_{mw} and t_{j} are mean winter and mean January air temperatures, °C; t_{s} is mean annual soil temperature without snow and vegetation cover, °C.

* After [Dereviagin *et al.*, 2007].

Table 4. Paleoreconstructions based on $\delta^{18}\text{O}_{\text{iw}}$ data for Late Pleistocene and Holocene syngenetic ice wedges in islands of Russian East Arctic, modified and complemented after [Vasil'chuk, 1992]*

Reference section	Paleoreconstructions					Modern values					
	$\delta^{18}\text{O}_{\text{iw}}$, ‰	Σt_w°	t_{mw}°	t_j°	t_s	$\delta^{18}\text{O}_{\text{iw}}$, ‰	Σt_w°	t_{mw}°	t_j°	t_s	
	<i>50–45 Kyr BP</i>										
Kotelny Island**	–29.5	–7400	–30	–44	–18	–18	–5408	–19	–29	–13	
Bolshoy Lyakhovsky Island	–30.0	–7500	–30	–45	–18	–20	–5400	–20	–31	–14	
	<i>35–25 Kyr BP</i>										
Kotelny Island	–29.0	–7250	–29	–43	–19	–18	–5408	–19	–29	–13	
Zhokhov Island	–28.5	–7150	–28	–43	–19	–20	–5363	–18	–29	–13	
Bolshoy Lyakhovsky Island	–31.5	–7870	–32	–48	–20	–20	–5400	–20	–31	–13	
Ayon Island	–31.0	–7750	–31	–46	–19	–21	–5047	–20	–29	–12	
	<i>22–12 Kyr BP</i>										
Kotelny Island	–25.0	–6250	–25	–37	–16	–18	–5408	–19	–29	–13	
Ayon Island	–29.5	–7400	–30	–44	–18	–21	–5047	–20	–29	–12	
	<i>9–2 Kyr BP</i>										
Kotelny Island	–22.5	–5600	–22	–34	–13	–18	–5408	–19	–29	–13	
Bolshoy Lyakhovsky Island	–24.5	–6100	–24	–36	–15	–20	–5400	–20	–31	–14	
Maly Lyakhovsky Island	–21.0	–5500	–21	–32	–13	–18	–5408	–20	–31	–14	
Zhokhov Island	–21.0	–5300	–21	–32	–11	–20	–5363	–18	–29	–13	
Ayon Island	–22.0	–5400	–22	–33	–12	–21	–5047	–20	–29	–12	

* Isotope data on ice wedges are complemented by data from [Meyer et al., 2002] for Bolshoy Lyakhovsky Island and from [Pavlova et al., 2009] for Zhokhov Island.

** After [Schirmeister et al., 2003; Dereviagin et al., 2007].

counterparts from 22–12 Kyr BP suggesting less severe winters, which was also reported for several reference permafrost sections in Siberia [Vasil'chuk, 1992, 2006]. The Holocene ice wedges show more positive $\delta^{18}\text{O}$ values than the Late Pleistocene ones in the New Siberian Islands and in the Lena mouth and, correspondingly, 5–7 °C warmer mean winter air temperatures than in Kotelny. The 50–45 Kyr BP Kotelny ice wedges have the most negative $\delta^{18}\text{O}$ values (–29.5 ‰) of the whole data series for the island.

The pollen spectra in 36.6–35.5 cal. Kyr BP samples indicate vegetation conditions favorable for the growth of larch and birch. Taking into account the available 47.6–39.5 cal. Kyr BP ^{14}C ages of wood from Kotelny Island [Galanin et al., 2015], we may infer that there were at least two warm excursions with better vegetation conditions in the area: from 47 to 39 and from 36.6 to 35.5 Kyr BP. Such spells of climate optimum existed during MIS-3 between 48 and 38 cal. Kyr BP in Bolshoy Lyakhovsky Island and from 40 to 32 cal. Kyr BP in the Lena Delta [Wetterich et al., 2014]. The 35–25 Kyr BP ice wedge samples show –29.0 ‰ $\delta^{18}\text{O}$ on average.

The pollen spectra of peatland that formed from 34 to 29 cal. Kyr BP [Lozhkin, 1977] record mosaic patterns of vegetation including shrubs. Determinations for seed remnants show much better conditions for vegetation than at present. The island was grown with lowland grass-hypnum communities in the 28–

26 cal. Kyr BP interval and eutrophic herb-hypnum and hypnum tundra vegetation grew from 26 to 23 cal. Kyr BP at high or periodically excess moisture [Pavlova et al., 2009]. In 22–12 Kyr BP, average $\delta^{18}\text{O}$ was –25.0 ‰. Drier conditions from 23 to 19 cal. Kyr BP in Kotelny Island are recorded in pollen spectra with predominant Poaceae and Poaceae-*Artemisia* pollen and some species of open stony landscapes [Makeev et al., 1989; Pavlova et al., 2009]. The respective spectra for 19.0–14.5 cal. Kyr BP containing *Artemisia* and Poaceae pollen easily transported by wind show patchy vegetation patterns and very low pollen productivity of plants; *Artemisia*-Poaceae and *Artemisia* communities may have predominated locally. After 14.5–12.5 ca. Kyr BP, the vegetation of the island consisted of sedge-herb communities [Makeev et al., 1989, 2003], with open stony patches. In the Late Pleistocene (11.0–2.5 cal. Kyr BP), the *Artemisia*-Poaceae and Poaceae phytocenoses gave way to Poaceae-Cyperaceae-grass tundra vegetation with more abundant shrub-grass and grass-shrub tundra communities.

In the 9–2 Kyr BP interval, ice wedge samples show an average $\delta^{18}\text{O}$ value of –22.5 ‰, while the pollen spectra reveal three events in the vegetation history [Makeev et al., 2003]. The division suggested by D. Ponomareva [Makeev et al., 2003] is as follows: low summer air temperatures and lesser percentages of shrubs in 9–8 Kyr BP; better conditions favorable

for tall shrubs followed by summer cooling and spread of *Artemisia*-Poaceae communities with dwarf birch from 8 to 5 Kyr BP; and vegetation similar to the present one, with patches of dwarf birch among Poaceae-Cyperaceae tundra communities after 5 Kyr BP.

CONCLUSIONS

1. $\delta^{18}\text{O}$ value variations in Late Pleistocene ice wedges in Kotelny Island exceed 6 ‰, which is evidence of large variability of winter air temperatures of that time. Mean monthly January temperature variations were above 10 °C.

2. A Late Pleistocene ice wedge encloses a Holocene ice wedge intruded from above, which is a very rare phenomenon.

3. Relatively stable oxygen isotope compositions of Holocene ice wedges (ranges not exceeding 2 ‰ $\delta^{18}\text{O}$) indicate stable winter air temperatures in the island area: long-term mean January air temperature variations in the Holocene were within 3 °C.

4. The Late Pleistocene climate history included several excursions with quite high summer temperatures and long vegetation periods, which maintained patchy growth of trees and tall shrubs in the island from 47 to 39 and from 36.6 to 35.5 Kyr BP.

5. In the earliest Holocene (10–7 Kyr BP), the conditions in the island were favorable for tall shrub growth and rapid peat deposition.

6. Winters during the cold spells of the Karga period were markedly colder but the vegetation period was more favorable than those during the Sartan period.

We wish to thank Dr. Ju. Chizhova for aid in isotope determinations and for useful advice. Thanks are extended to Prof. R. Vaikmäe, for performing isotope analytical work, Dr. N. Belova for offering photographs, and B. Petrov for assistance in sampling the Holocene section in Kotelny Island.

The work was sponsored by grants 8-05-60272 Arctic; 17-05-00794, and 17-05-00793 from the Russian Foundation for Basic Research and additionally supported by government funding to Moscow State University. Mass spectrometry equipment was purchased as part of a Moscow State University development program.

References

- Anisimov, M.A., 2010. The Holocene Climate and Environment of the New Siberian Archipelago. Author's Abstract, Candidate Thesis (Geography). St. Petersburg, 24 pp. (in Russian)
- Belova, N.G., Frolov, D.M., Kizyakov, A.I., Konstantinova, N.G., 2015. Ice complex on the southern coast of Kotelny Island, New Siberian Islands: New data on isotopic composition, in: Permafrost in XXI Century: Basic and Applied Research, Proc. Intern. Conf., Pushchino, Moscow Region, Russia, pp. 123–125.
- Bronk Ramsey, C., 2009. Bayesian analysis of radiocarbon dates. *Radiocarbon* 51 (1), 337–360.
- Climate of Kotelny Island. <http://www.pogodaiklimat.ru/climate/21432.htm> (last visited 22.05.2018).
- Dereviagin, A.Yu., Kunitsky, V.V., Meyer, H., 2007. Composite wedges in the North of Yakutia. *Kriosfera Zemli* XI (1), 62–71.
- Dobrowolska, K., 2014. Weather types at selected meteorological stations in Siberia. *Bull. Geography. Phys. Geogr. Ser.* 7, 81–104.
- Galanin, A.A., Dyachkovskiy, A.P., Lytkin, V.M., Burnasheva, M.P., Shaposhnikov, G.I., Kut', A.A., 2015. Absolute ages of samples determined at the Radiocarbon Laboratory at the Institute of Permafrost (Yakutsk). *Nauka i Obrazovanie*, No. 4, 45–49.
- Gorodkov, B.N., 1948. Pleistocene periglacial landscapes in northern Asia. *Dokl. AN SSSR* 61 (3), 513–516.
- Gorodkov, B.N., 1956. Vegetation and soils of Kotelny Island (New Siberian Archipelago), in: Tikhomirov, B.A. (Ed.), *The Vegetation and Land Use in the USSR Far North*, Iss. 2, USSR Academy Publishers, Leningrad, pp. 7–132. (in Russian)
- Grichuk, V.P., Fedorova, R.V., 1956. On Quaternary periglacial vegetation in northern Asia. *Izv. AN SSSR, Ser. Geogr.* No. 2, 66–71.
- Kachinskii, V.L., 2014. Industrial Hydrocarbons in Arctic Tundra Soils of Bolshoy Lyakhovskiy Island, New Siberian Archipelago. Candidate Thesis (Geography), Moscow, 176 pp. (in Russian)
- Kienast, F., Wetterich, S., Kuzmina, S., Schirrmeister, L., Andreev, A.A., Taresov, P., Nazarova, L., Kossler, A., Frolova, L., Kunitsky, V.V., 2011. Paleontological records indicate the occurrence of open woodlands in a dry inland climate at the present-day Arctic coast in Western Beringia during the Last Interglacial. *Quatern. Sci. Rev.* 30 (17–18), 2134–2159.
- Lozhkin, A.V., 1977. Radiocarbon ages of Late Pleistocene deposits in the New Siberian Islands and the age of ice complexes in northeastern USSR. *Dokl. AN SSSR* 235 (2), 435–437.
- Lozhkin, A.V., 2002. Modern pollen rain in Arctic Beringia and vegetation reconstructions for glacial periods of the Pleistocene, in: *Quaternary Paleogeography of Beringia*. SVKNII DVO RAN, Magadan, pp. 13–27. (in Russian)
- Makeev, V.M., Arslanov, Kh.A., Baranovskaya, O.F., Kosmodamiansky, D.P., Tertychnaya, T.V., 1989. Late Pleistocene and Holocene stratigraphy, geochronology, and paleogeography of Kotelny Island. *Bull. Quaternary Commission* 58, pp. 58–69.
- Makeev, V.M., Ponomareva, D.P., Pitulko, V.V., Chernova, G.V., Solovyeva, D.V., 2003. Vegetation and climate of the New Siberian Islands for the past 15,000 years. *Arctic, Antarctic, and Alpine Res.* 35, 56–66.
- Meyer, H., Dereviagin, A., Siegert, C., Schirrmeister, L., Hubberten, H.-W., 2002. Palaeoclimate reconstruction on Big Lyakhovsky Island, North Siberia – hydrogen and oxygen isotopes in ice wedges. *Permafrost and Periglacial Processes* 13 (2), 91–105.
- Morizumi, J., Iida, T., Fukuda, M., 1995. Radiocarbon dating of methane obtained from air in the ice complex (edoma), in Arctic coast area of east Siberia, in: Tsukuba, K., Takahashi, A., Osawa, Y., Kanazawa (Eds.), *Joint Siberian Permafrost Studies between Japan and Russia in 1994: Proc. Third Intern. Symp., Hokkaido, Japan, Hokkaido Univ. Press*, pp. 14–21.

- Opel, T., Wetterich, S., Meyer, H., Derevyagin, A.Y., Fuchs, M.C., Schirrmeister, L., 2017. Ground-ice stable isotopes and cryostratigraphy reflect late Quaternary palaeoclimate in the Northeast Siberian Arctic (Oyogos Yar coast, Dmitry Laptev Strait). *Climate of the Past* 13, 587–611.
- Pavlova, E.Yu., Dorozhkina, M.V., Pitulko, V.V., 2009. The latest Late Pleistocene climate and environment of the Anjou Islands: Paleogeographic reconstructions, in *Global Arctic and Subarctic Geology, Proc. XLII Tectonic Conf. Volume 2*, pp. 97–101. (in Russian)
- Pavlova, E.Yu., Ivanova, V.V., Meyer, H., Pitulko, V.V., 2015. The oxygen isotope composition of fossil ice as a climate proxy: case study of the northern New Siberian Islands and the western Yana-Indigirka lowland, in: *Proc. IX All-Russian Conf. on the Quaternary, 15–20 September 2015, Irkutsk*, V.B. Sochava Institute of Geography, Irkutsk, pp. 349–351. (in Russian)
- Reimer, P.J., Bard, E., Bayliss, A., Beck, J.W., Blackwell, P.G., Ramsey, C.B., Buck, C.E., Cheng, H., Edwards, R.L., Friedrich, M., Grootes, P.M., Guilderson, T.P., Haffidason, H., Hajdas, I., Hatté, C., Heaton, T.J., Hoffmann, D.L., Hogg, A.G., Hughen, K.A., Kaiser, K.F., Kromer, B., Manning, S.W., Niu, M., Reimer, R.W., Richards, D.A., Scott, E.M., Southon, J.R., Staff, R.A., Turney, C.S.M., van der Plicht, J., 2013. IntCal13 and Marine13 Radiocarbon age calibration curves 0–50,000 years cal BP. *Radiocarbon* 55 (4), 1869–1887.
- Remnants of a small mammoth discovered in Kotelnny Island in Yakutia, 2018. <http://news.ykt.ru/mobile/article/76179> (last visited 08.10.2018).
- Schirrmeister, L., Siegert, C., Kuznetsova, T., Kuzmina, S., Andreev, A., Kienast, F., Meyer, Y., Bobrov, A., 2002. Paleoenvironmental and paleoclimatic records from permafrost deposits in the Arctic region of Northern Siberia. *Quatern. Intern.* 89 (1), 97–118.
- Schirrmeister, L., Grosse, G., Kunitsky, V., Meyer, H., Derevyagin, A., Kuznetsova, T., 2003. Permafrost, periglacial and paleo-environmental studies on New Siberian Islands, in: Grigoriev, M.N., Rachold, V., Bolshiyarov, A.Y., Pfeiffer, E.-M., Schirrmeister, L., Wagner, D., Hubberten, H.-W. (Eds.). *Russian-German Cooperation System Laptev Sea. The expedition Lena 2002. Berichte zur Polar- und Meeresforschung. Rep. on Polar and Marine Res.* 466, pp. 195–261.
- Schirrmeister, L., Kunitsky, V., Grosse, G., Wetterich, S., Meyer, H., Schwamborn, G., Babiy, O., Derevyagin, A., Siegert, C., 2011. Sedimentary characteristics and origin of the Late Pleistocene ice complex on north-east Siberian Arctic coastal lowlands and islands – A review. *Quatern. Intern.* 241 (1–2), 3–25.
- Ship History of Russia. <http://shiphistory.ru/> Appeal 20 November 2018. (in Russian)
- Sulerzhitsky, L.D., Romanenko, E.A., 1997. Age and distribution of the mammoth fauna of the polar region of Asia (radiocarbon dating results). *Kriosfera Zemli* I (4), 12–19.
- Toll, E., 1897. Fossil glaciers of New Siberian Islands, their relation to mammoth corpses and to the glacial period, from data of two expeditions of 1885–1886 and 1893, supported by the Imperial Academy of Sciences, in: Mushketov, I.V. (Ed.), *Reports, Imperial Russian Geographical Society, General Geography, St. Petersburg* 32 (1), 139 pp. (in Russian)
- Troshko, K.A., 2018. Use of Radar Data for Thematic Mapping: Methodological Development. Author's Abstract, Candidate Thesis (Geography). Moscow University, Moscow, 22 pp. (in Russian)
- van Geel, B., Protopopov, A., Protopopova, V., Pavlov, I., van der Plicht, J., van Reenen, G.B.A., 2017. *Larix* during the Mid-Pleniglacial (Greenland Interstadial 8) on Kotelnny Island, northern Siberia. *Boreas* 46 (2), 338–345, DOI: 10.1111/bor.12216.
- Vasil'chuk, A.C., 2003. Appearance of Heinrich events in radiocarbon dated pollen diagrams of ice wedges and its surrounding yedoma sediments of the lower Kolyma River. *Kriosfera Zemli* VII (4), 3–13.
- Vasil'chuk, Yu.K., 1988. Paleological permafrost interpretation of oxygen isotope composition of Late Pleistocene and Holocene wedge ice of Yakutia. *Transactions (Doklady) of the USSR Academy of Sciences: Earth Sci. Sections* 298 (1), 56–59 (Publ. by Scripta Technica, Inc. A Wiley Company, N.Y.).
- Vasil'chuk, Yu.K., 1991. Reconstruction of the palaeoclimate of the Late Pleistocene and Holocene of the basis of isotope studies of subsurface ice and waters of the permafrost zone. *Water Resources* 17 (6), 640–647.
- Vasil'chuk, Yu.K., 1992. Oxygen Isotope Composition of Ground Ice (Application to Paleogeocryological Reconstructions), *Theor. Probl. Dept., RAS, Moscow University, Research Institute of Engineering for Construction (PNIIS)*, Moscow, Book 1, 420 pp., Book 2, 264 pp. (in Russian)
- Vasil'chuk, Yu.K., 2006. *Ice Wedge: Heterocyclity, Heterogeneity, Heterochronicity*. Moscow University Press, Moscow, 404 pp. (in Russian)
- Vasil'chuk, Yu.K., Makeev, V.M., Maslakov, A.A., Budantseva, N.A., Vasil'chuk, A.C., 2016. Paleogeocryological conditions of Late Pleistocene and Holocene ice wedges in Kotelnny Island, in: *Proc. 5th Conf. of Russian Geocryologists*, Moscow, 14–17 June, 2016. *Univ. Kniga, Volume 2*, pp. 284–291. (in Russian)
- Vasil'chuk, Yu.K., Makeev, V.M., Maslakov, A.A., Budantseva, N.A., Vasil'chuk, A.C., Chizhova, Ju.N., 2018. The oxygen isotope composition of Late Pleistocene and Holocene ice wedges of Kotelnny Island. *Doklady Earth Sci.* 482 (1), 1216–1220, DOI: 10.1134/S1028334X18090192.
- Vasil'chuk, Yu.K., Vasil'chuk, A.C., 2018. Winter air paleotemperatures at 30–12 Ka BP in the lower Kolyma River, Plakhinskii Yar Yedoma: Evidence from stable isotopes. *Earth's Cryosphere (Kriosfera Zemli)* XXII (5), 3–16.
- Wetterich, S., Tumskey, V., Rudaya, N., Andreev, A.A., Opel, T., Meyer, H., Schirrmeister, L., Hüls, M., 2014. Ice Complex formation in arctic East Siberia during the MIS3 Interstadial. *Quatern. Sci. Rev.* 84, 39–55.
- Zimmermann, H.H., Raschke, E., Epp, L.S., Stoof-Leichsenring, K.R., Schirrmeister, L., Schwamborn, G., Herzschuh, U., 2017. The history of tree and shrub taxa on Bol'shoy Lyakhovsky Island (New Siberian Archipelago) since the last interglacial uncovered by sedimentary ancient DNA and pollen data. *Genes* 8 (273), 28 pp.

Received June 20, 2018

Revised version received November 6, 2018

Accepted November 28, 2018